

## Structural and compositional dependences of the Schottky barrier in Al/Ga<sub>1-x</sub>Al<sub>x</sub>As(100) and (110) junctions

J. Bardi, N. Binggeli, and A. Baldereschi

*Institut de Physique Appliquée, École Polytechnique Fédérale de Lausanne, CH-1015 Lausanne, Switzerland*

(Received 31 August 1998)

Based on *ab initio* pseudopotential calculations, we have examined the equilibrium atomic geometries and electronic structure of chemically abrupt epitaxial Al/GaAs and Al/Ga<sub>1-x</sub>Al<sub>x</sub>As(100) and (110) interfaces. In particular, we investigated the change in the corresponding Schottky barrier height for different interface atomic geometries and semiconductor alloy compositions. Our results indicate that different epitaxial geometries and orientations of the interface can change the absolute value of the Schottky barrier by as much as 0.4 eV. However, for a given equilibrium geometry of the interface, Al/Ga<sub>1-x</sub>Al<sub>x</sub>As(100) and (110) junctions exhibit compellingly similar barrier variations with alloy composition, which amount to the GaAs/Ga<sub>1-x</sub>Al<sub>x</sub>As band offset. The observed trend is explained on the atomic scale using a linear-response-theory approach. [S0163-1829(99)07811-X]

### I. INTRODUCTION

Although metal/semiconductor interfaces have been studied for several decades, the mechanisms of Schottky-barrier formation are still far from being completely elucidated.<sup>1</sup> Until recently, most measurements of Schottky barriers in metal/III-V-semiconductor junctions indicated a relatively weak dependence of the barrier height on the metal type or on interface-specific characteristics such as interface orientation or contact fabrication method. Models of Schottky-barrier formation were proposed that explained this behavior based on various Fermi-level pinning mechanisms, such as pinning by metal-induced gap states<sup>2</sup> at an intrinsic charge neutrality level of the semiconductor,<sup>3,4</sup> or pinning by native defect states at some extrinsic gap level.<sup>5,6</sup> Moreover, a correlation between Schottky barriers and heterojunction band offsets was observed experimentally for a number of systems.<sup>7</sup> These included contacts to III-V alloys such as Al/Ga<sub>1-x</sub>Al<sub>x</sub>As, CoGa/Ga<sub>1-x</sub>Al<sub>x</sub>As,<sup>8</sup> Mo/Ga<sub>1-x</sub>Al<sub>x</sub>As, Au/Ga<sub>1-x</sub>Al<sub>x</sub>As,<sup>7</sup> and Au/In<sub>1-x</sub>Ga<sub>x</sub>As<sub>1-y</sub>P<sub>y</sub> lattice matched to GaAs,<sup>9</sup> which exhibit Schottky barrier variations with semiconductor alloy composition identical to that of the corresponding GaAs/Ga<sub>1-x</sub>Al<sub>x</sub>As or GaAs/In<sub>1-x</sub>Ga<sub>x</sub>As<sub>1-y</sub>P<sub>y</sub> band offsets. This behavior was also interpreted in terms of band alignment controlled by pinning of bulk reference levels.<sup>10</sup>

In recent years, however, significant variations of the Schottky barrier with metallization and/or with surface or interface preparation were reported.<sup>11-13</sup> For instance, differences as large as 0.4 eV were found between the values of the Schottky barrier measured at Al/GaAs(110) contacts grown by metal cluster deposition and those measured in junctions grown by conventional deposition methods.<sup>11</sup> Even larger barrier changes, approaching 1 eV, were demonstrated in Al/GaAs(100) junctions containing ultrathin Si interlayers.<sup>13</sup> These recent developments reveal a much weaker electronic pinning than previously believed and emphasize the role of the interface atomic structure in determining the Schottky barrier height.

In the present study, we use first principles calculations to clarify some of these contrasting behaviors for the prototype Al/Ga<sub>1-x</sub>Al<sub>x</sub>As system. The existence of good lattice matching between Al and Ga<sub>1-x</sub>Al<sub>x</sub>As, which gives rise to quasiepitaxial Al/Ga<sub>1-x</sub>Al<sub>x</sub>As(100) (Refs. 14-16) and Al/GaAs(110) contacts,<sup>17</sup> allows first-principles investigations of fully developed metal/semiconductor interfaces. Previous *ab initio* studies examined the electronic structure of epitaxial Al/GaAs junctions using as a starting atomic geometry a configuration derived from the juxtaposition of truncated bulk structures aligned so that some of the metal-surface ions occupy atomic sites in the continuation of the semiconductor lattice.<sup>18-21</sup> These pioneering studies showed that substantial changes in the Schottky barrier could be induced altering the atomic structure of the interface. Systematic investigations of the energetics and relative stability of different types of epitaxial configurations are, however, much more scarce. Needs *et al.* examined the formation energies of various Al/GaAs(110) epitaxial structures obtained by translating the metal overlayer parallel to the semiconductor surface.<sup>22</sup> The results indicated that the lowest-energy structure differed from previous atomistic models<sup>18,19</sup> and that the Schottky barrier could change dramatically with the translation state.

In this paper, we focus on the epitaxial Al/Ga<sub>1-x</sub>Al<sub>x</sub>As(100) and (110) junctions, and study the dependence of the Schottky barrier height on the semiconductor alloy composition as well as on the interface geometry. To determine the epitaxial structures, we carried out a systematic study of atomic relaxation and relative stability of various translation states for both the Al/GaAs(100) and (110) junctions. For the polar Al/GaAs(100) junctions, we found a unique equilibrium interfacial configuration for a given cation or anion termination of the semiconductor surface, consistent with previous atomistic models. For the Al/GaAs(110) junctions, instead, we obtained a series of structures characterized by different interfacial bonds. In contrast to previous work,<sup>22</sup> we find that these structures are all essentially degenerate in energy and give rise to relatively similar Schottky barrier heights when the atomic structure at

the interface is fully relaxed. Together, our results for Al/Ga<sub>1-x</sub>Al<sub>x</sub>As(100)- and (110)-oriented junctions show that although the absolute value of the Schottky barrier depends on the atomic structure and orientation of the interface, for a given orientation and equilibrium geometry of the interface, the variation of the barrier with semiconductor alloy composition  $x$  essentially follows the GaAs/Ga<sub>1-x</sub>Al<sub>x</sub>As band offset. This behavior is explained on the atomic scale by extending to metal/semiconductor interfaces a linear-response-theory approach currently used to interpret band-offset trends at semiconductor heterojunctions.<sup>23</sup>

## II. METHOD

The calculations were performed within the local-density approximation (LDA) to density-functional theory (DFT) using Troullier-Martins pseudopotentials<sup>24</sup> in the Kleinman-Bylander nonlocal form.<sup>25</sup> We employed the exchange-correlation functional by Ceperley and Alder.<sup>26</sup> The electronic wave functions were expanded in a plane-wave basis set, which allows for a convenient momentum-space formulation.<sup>27</sup> To describe the alloying on the cation sublattice in Ga<sub>1-x</sub>Al<sub>x</sub>As, we used the virtual-crystal approximation<sup>28</sup> and we treated Ga<sub>1-x</sub>Al<sub>x</sub>As as lattice matched to GaAs.

The isolated metal/semiconductor interfaces were simulated using a slab geometry in supercells characterized by two integers,  $n+m$ , corresponding to the number of semiconductor and metal layers, respectively. Most of our calculations were performed using a 9+7 supercell for the (110) orientation and a 13+7 supercell for the (100) orientation. We employed, however, larger supercells to study the effect of Ga→Al atomic substitutions performed near the interface in Al/GaAs (100) and (110) junctions (Sec. IV C). For such calculations we used a 15+7 supercell for the (110) junction and a 21+7 supercell for the (100) junction. All supercell computations were carried out with a kinetic-energy cutoff of 16 Ry. For the Brillouin-zone (BZ) integrations we used (6, 6, 2) and (6, 4, 2) Monkhorst-Pack (MP) grids for the (100) and (110) interfaces, respectively. A Gaussian broadening scheme, with a full width at half maximum of 0.1 eV, was used to deal with the partial filling of the bands.<sup>29</sup> The relaxed atomic positions at the interfaces were obtained by total-energy minimization using the Hellmann-Feynman forces.

As often done in band alignment problems, we split the Schottky barrier height into two parts:<sup>23,30</sup>

$$\phi_p = \Delta E_p + \Delta V. \quad (1)$$

The first part  $\Delta E_p$  is the difference between the Fermi level of the metal  $E_F$  and the valence-band edge of the semiconductor  $E_v$ , each measured with respect to the (ill-defined and set to zero in the bulk calculations) average electrostatic potential in the corresponding crystal. We evaluated  $\Delta E_p$  from two separate bulk band-structure calculations performed with a 40-Ry cutoff, and using the (16, 16, 16) and (8, 8, 8) MP grids to sample the charge density of the metal and semiconductor, respectively. The second term  $\Delta V$  is the difference between the average electrostatic potentials in the two materials, far from the interface. This term contains all interface-specific contributions to  $\phi_p$ .  $\Delta V$  was derived via Poisson's

equation from the self-consistent supercell charge density using the techniques of the planar and macroscopic averages.<sup>23</sup>

Our LDA values for the Schottky barriers are subject to some *a posteriori* corrections due to (i) many-body effects, (ii) spin-orbit interactions, and (iii) semicore-orbital effects. Many-body corrections to the LDA band-edge energy  $E_v$  have been evaluated from self-energy calculations for GaAs in Refs. 22 and 31, and for AlAs in Ref. 31. Two different values were reported for GaAs:  $\Delta E_v^{\text{GaAs}} = -0.36$  eV (Ref. 22) and  $-0.17$  eV (Ref. 31). The difference is due, most likely, to the fact that different exchange-correlation functionals were used in the two studies. We decided to use the value of Ref. 22, which corresponds to the same exchange-correlation functional as employed in our study. The many-body correction for AlAs was included using the correction for GaAs, and the difference between the GaAs and AlAs corrections as evaluated in Ref. 31, i.e.,  $\Delta E_v^{\text{GaAs}} - \Delta E_v^{\text{AlAs}} = 0.1$  eV. The latter result is the commonly accepted value for the many-body correction on the AlAs/GaAs valence-band offset (VBO).<sup>23</sup> In principle, no self-energy correction is required for the Fermi energy of the metal  $E_F$ , which should be correctly described by the highest occupied eigenvalue within DFT.<sup>32</sup> In fact, similar LDA-DFT calculations performed with the same Al pseudopotential as in the present study yield work functions for the three main surface orientations of Al, which agree to within a few tenths of meV with experiment.<sup>33</sup> In this paper, we therefore use for  $E_F$  the bare LDA-DFT result.<sup>34</sup>

The spin-orbit splitting  $\Delta_{\text{SO}}$  of the semiconductor valence-band edge, neglected in our scalar-relativistic calculations, decreases  $\Delta E_p$  by  $\frac{1}{3}\Delta_{\text{SO}}$ . Using the experimental value of  $\Delta_{\text{SO}}$ , this yields a spin-orbit correction of  $-0.11$  eV ( $-0.09$  eV) on  $\phi_p$  for Al/GaAs (Al/AlAs). We have studied in detail the effects of the semicore Ga 3*d* electrons on the Al/GaAs Schottky barrier in the case of a (100)-oriented junction (see the Appendix). We show in the Appendix that the Ga 3*d* effects can be considered as a *bulk* correction, which raises the top of the valence band in GaAs by 0.1 eV. We note that this correction also takes into account the increase in the GaAs equilibrium lattice parameter due to the presence of the Ga 3*d* electrons, which accounts for 50% of the shift. The same increase in the AlAs lattice parameter also decreases  $\phi_p(\text{Al/AlAs})$  by 0.05 eV. In the following, we therefore treat the Ga 3*d* orbitals as core states, and use a rigid correction of  $-0.10$  eV on  $\phi_p(\text{Al/GaAs})$  to take into account the Ga 3*d* effects and a correction of  $-0.05$  eV on  $\phi_p(\text{Al/AlAs})$  to take into account the corresponding change in the AlAs lattice parameter. The corrections (i) to (iii) described above are bulk corrections, independent of the atomic structure and orientation of the interface. They sum up to a global correction of  $+0.15$  eV on  $\phi_p(\text{Al/GaAs})$  and  $+0.32$  eV on  $\phi_p(\text{Al/AlAs})$ . For  $\phi_p(\text{Al/Ga}_{1-x}\text{Al}_x\text{As})$  with  $0 < x < 1$ , we use a linear interpolation between these two values.

The estimated uncertainty on the absolute value of  $\phi_p$  taking into account the various corrections is  $\sim 0.1$  eV. However, for the relative values of the Schottky barriers the estimated uncertainty is of the order of our numerical accuracy, i.e.,  $\sim 40$  meV. Similarly, for the absolute value of our computed formation energies, we estimate the uncertainty as

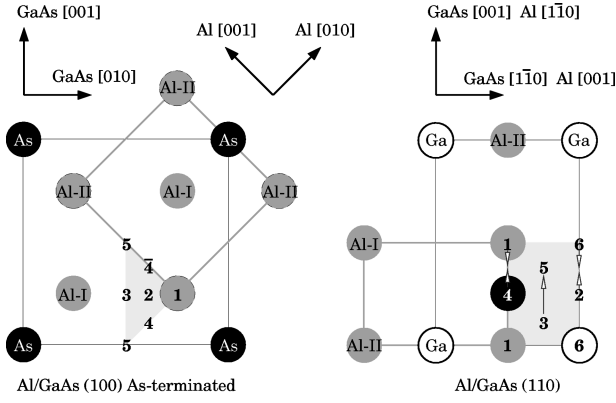


FIG. 1. Epitaxial geometries of the As-terminated Al/GaAs (100) interface (left panel) and Al/GaAs (110) interface (right panel). Different translation states (TS) are obtained by rigidly displacing the Al overlayer parallel to the semiconductor surface. The TS's considered in this paper are indicated by numbers, which show the projected position of an Al ion of the first metal layer on the semiconductor surface. The shaded area shows the irreducible zone of the translation states. The labels used for the (110) TS's are the same as in Ref. 22 and the arrows indicate, for each TS, the displacement of the Al slab (central layer) relative to the GaAs slab after relaxation (see text).

0.2 eV per surface atom, whereas the estimated accuracy on the relative values of the formation energies for the various interface configurations is of the order of 0.01 eV per surface atom.

### III. ENERGETICS AND STRUCTURAL PROPERTIES OF EPITAXIAL Al/GaAs JUNCTIONS

#### A. Lattice alignment at abrupt (100) and (110) interfaces

The Al and GaAs equilibrium lattice parameters verify experimentally within 1.3%—within 1.5% in our calculations—the epitaxial condition:  $a_{\text{Al}} = a_{\text{GaAs}}/\sqrt{2}$ . This means that an Al (100) overlayer may be grown epitaxially on a GaAs (100) substrate with the Al fcc lattice rotated by  $45^\circ$  about the  $[100]$  axis with respect to the GaAs cubic lattice. In the case of a GaAs (110) substrate, an epitaxial structure may be obtained with an Al (110) overlayer rotated by  $90^\circ$  about the  $[110]$  axis with respect to the GaAs lattice. These two types of epitaxial structures have been observed experimentally,<sup>15,17</sup> and atomistic models corresponding to abrupt junctions are presented in Fig. 1 for these two types of interfaces.

Following macroscopic elasticity theory, the lattice mismatch is accommodated, in such pseudomorphic structures, by a deformation of the Al overlayer along the growth direction, corresponding to a lattice constant  $a_\perp$  given by

$$a_\perp^{(100)} = a_{\text{Al}} \left[ 1 - 2 \frac{C_{12}}{C_{11}} \left( \frac{a_\parallel}{a_{\text{Al}}} - 1 \right) \right], \quad (2)$$

$$a_\perp^{(110)} = a_{\text{Al}} \left[ 1 - \frac{C_{11} + 3C_{12} - 2C_{44}}{C_{11} + C_{12} + 2C_{44}} \left( \frac{a_\parallel}{a_{\text{Al}}} - 1 \right) \right], \quad (3)$$

where  $a_\parallel = a_{\text{GaAs}}/\sqrt{2}$  is the Al in-plane lattice constant and  $C_{ij}$  are the Al elastic constants.

In our study, we used the theoretical equilibrium lattice parameters  $a_{\text{GaAs}} = 5.53 \text{ \AA}$ ,  $a_{\text{Al}} = 3.97 \text{ \AA}$  ( $a_\parallel = 3.91 \text{ \AA}$ ), and the calculated elastic constants:  $C_{11} = 120 \text{ GPa}$ ,  $C_{12} = 70 \text{ GPa}$ , and  $C_{44} = 36 \text{ GPa}$ . The experimental values are:  $a_{\text{GaAs}}^{\text{exp}} = 5.65 \text{ \AA}$ ,  $a_{\text{Al}}^{\text{exp}} = 4.05 \text{ \AA}$ ,  $C_{11}^{\text{exp}} = 114 \text{ GPa}$ ,  $C_{12}^{\text{exp}} = 62 \text{ GPa}$ , and  $C_{44}^{\text{exp}} = 32 \text{ GPa}$ .<sup>35</sup> The theoretical values of the Al elastic constants were determined from the stress/strain dependence using a 40-Ry cutoff and up to  $\sim 2000$  irreducible points in the BZ. The stresses were found to depend linearly on strain for deformations up to 1.5%. The resulting lattice constants of the Al(100) and (110) overlayers along the growth direction are  $a_\perp^{(100)} = 4.05 \text{ \AA}$  and  $a_\perp^{(110)} = 4.04 \text{ \AA}$ .

In order to fully specify the lattice alignment at the unrelaxed abrupt interfaces, additional information is needed on the relative position of the first Al layer with respect to the last semiconductor plane. This can be done by specifying the corresponding interplanar distance as well as the translation state (TS) parallel to the semiconductor surface of the Al layer. The interplanar distance at the interface determines— together with  $a_{\text{GaAs}}$  and  $a_\perp$ —the length of our supercell. The five (100) and six (110) initial (unrelaxed) TS's considered in this paper and the irreducible wedges of the possible (100) and (110) TS's are shown in Fig. 1. For the (100) orientation, we considered both the As- and Ga-terminated GaAs (100) surfaces. For the interplanar distance, we used the bulk GaAs (110) interplanar distance for the Al/GaAs (110) junctions (2.0  $\text{\AA}$ ) and the average of the bulk GaAs (100) and Al (100) interplanar distances for the Al/GaAs (100) junctions (1.7  $\text{\AA}$ ). These values are close to the optimal values of the interfacial distance that we obtain from total energy calculations for the lowest-energy TS's, namely  $\sim 2.1 \text{ \AA}$  in the (110) junctions (for the TS1, TS2, and TS5 structures) and  $\sim 1.8 \text{ \AA}$  in the (100) junctions (for the As- and Ga-terminated TS1 structures).

#### B. Atomic relaxation and relative stability of the translation states

In Table I, we present the formation energies of the As- and Ga-terminated Al/GaAs (100) interfaces for the five initial TS's. The formation energy  $E_f$  is given by

$$E_f = \frac{1}{2} \left( E_{\text{tot}} - \sum_i n_i \mu_i \right), \quad (4)$$

where  $E_{\text{tot}}$  is the total energy of the supercell, and  $n_i$  and  $\mu_i$  are the number of atoms and the chemical potential for each atomic species  $i$  in the supercell. The factor  $\frac{1}{2}$  in Eq. (4) accounts for the fact that the supercell includes two equivalent interfaces.<sup>36</sup> The chemical potentials  $\mu_{\text{Al}}$  and  $\mu_{\text{GaAs}} = \mu_{\text{Ga}} + \mu_{\text{As}}$  are given by the total energies of the corresponding bulk material (strained in the case of Al) per unit cell. Since the supercells with the (100) orientation contain a different number of Ga and As atoms, the formation energy of their interfaces depends linearly on the isolated As (or Ga) chemical potential. The value of the As (Ga) chemical potential and the relative stability of the As- and Ga-terminated interfaces are normally determined by the experimental conditions. Here, as we are interested only in the relative stability of the different (100) TS's with a given cation or anion surface termination, we arbitrarily set the value of the As

TABLE I. Formation energy ( $E_f$ ) per semiconductor surface atom and  $p$ -type Schottky barrier height ( $\phi_p$ ) for the different translation states (TS) of the unrelaxed Al/GaAs (100) interface illustrated in Fig. 1. Results are given for the As and Ga terminations of the GaAs (100) surface. The last line gives the corresponding values for the relaxed lowest energy configuration (TS1'). For the TS4 (TS4) interface structures, the reported value of  $E_f$  is the average of the TS4 and TS4 formation energies (Ref. 36). A rigid correction of +0.15 eV should be added to the LDA values of the Schottky barriers to take into account relativistic, many-body and Ga 3d effects on the GaAs valence-band edge (see text).

Translation state	$E_f$ (eV)		$\phi_p^{(\text{LDA})}$ (eV)	
	As-term.	Ga-term.	As-term.	Ga-term.
TS1	0.78	1.20	0.64	0.51
TS2	1.08	1.63	0.65	0.52
TS3	1.48	2.13	0.65	0.52
TS4, TS4	2.16	2.60	0.57, 0.72	0.46, 0.52
TS5	5.75	5.56	0.50	0.35
TS1'	0.61	1.16	0.65	0.49

chemical potential to  $\mu_{\text{As}}^{\text{bulk}}$ , i.e., to the value in the As bulk-metallic phase (a choice corresponding to As-rich conditions). Another choice would simply rigidly shift the formation energies of the As-terminated junctions with respect to those of the Ga-terminated junctions.

Inspection of the formation energies in Table I and of the relative positions of the (100) TS's in Fig. 1 indicates that the only possible candidate for a (meta)stable interface structure is the TS1 geometry, both for the As- and Ga-terminated junctions. In both cases, the energy of the TS's increases with increasing displacement of the overlayer with respect to the TS1 configuration (from TS1 to TS2 and to TS3, and from TS1 to TS4 and TS5). In the favorable TS1 configuration, the atoms of the first Al layer occupy substitutional sites (Al-I) and tetrahedral interstitial sites (Al-II) in the continuation of the semiconductor zinc-blende lattice (see Fig. 1). The full relaxation of the atomic positions at the TS1 interface (configuration TS1' in Table I) lowers the formation energy by  $\sim 0.2$  eV for both terminations. This energy gain is related mainly to a buckling of the first Al layer, which reflects the different types of bonding of the Al-I and Al-II atoms to the semiconductor surface. The interplanar distance between the Al-I (Al-II) sublayer and the semiconductor surface decreases (increases), due to the increased covalent (metallic) character of the corresponding interfacial bonds. This behavior and the equilibrium atomic geometries of the As- and Ga-terminated interfaces are consistent with the results of a previous *ab initio* study by Dandrea and Duke, focusing on the TS1 configuration.<sup>20</sup>

We performed a similar analysis of the TS's for the (110) orientation. The formation energies of the (110) TS's are displayed in Table II. Although the irreducible wedge of the TS's is larger than in the case of the (100) orientation, the range of the formation energies for the unrelaxed configurations is significantly smaller. The three lowest energy configurations (TS1, TS2, and TS5), in particular, have very similar formation energies. When the atomic structure is allowed to relax, drastic changes are observed in the epitaxial geometry. The TS1 and TS4 structures collapse on an intermediate (TS1') configuration. Similarly, the TS2 and TS6 structures relax towards an intermediate (TS2') configuration, while the TS3 and TS5 structures relax towards a con-

figuration close to the TS5 structure (TS5'). Except for some local relaxation at the interface, most of the changes in the TS's can be described as a rigid displacement parallel to the interface of the Al slab with respect to the GaAs slab.<sup>37</sup> The corresponding in-plane displacements for the different TS's are indicated in Fig. 1. After relaxation, all of the TS's are essentially degenerate in energy (see Table II).

The relaxations of the TS4 and TS6 structures can be understood relatively easily based on the projected interface structures in Fig. 1. In the TS4 configuration, one half of the atoms of the first Al layer (Al-I) sit on top of the surface As atoms, while the other half (Al-II) are located on top of tetrahedral interstitial sites. This gives rise to ultrashort/extra long interfacial bonds between the Al-I/Al-II atoms and their As/Ga nearest neighbors. These unfavorable bonds are either shorter than 2 Å (As, Al-I) or longer than 3 Å (Ga, Al-II). The relaxation to the TS1' structure increases the length of the former to 2.40 Å, while reducing that of the latter to 2.74 Å. The situation is quite similar for the TS6 structure. In this case, the As and Ga atoms—and therefore the short and long bonds—are interchanged with respect to the TS4 structure. The relaxation to the TS2' structure increases the length of the short (Ga, Al-I) bonds to 2.46 Å, while reducing that of the long (As, Al-II) bonds to 2.72 Å.

TABLE II. Formation energy ( $E_f$ ) per GaAs pair and  $p$ -type Schottky barrier height ( $\phi_p$ ) for the different translation states (TS) of the Al/GaAs (110) interface described in Fig. 1. Results are given for unrelaxed and relaxed interface structures. A rigid correction of +0.15 eV should be added to the LDA values of the Schottky barriers to take into account relativistic, many-body and Ga 3d effects on the GaAs valence-band edge (see text).

Translation state	$E_f$ (eV)		$\phi_p^{(\text{LDA})}$ (eV)	
	Unrelaxed	Relaxed	Unrelaxed	Relaxed
TS1	1.79	1.24	0.67	0.27
TS2	1.68	1.27	0.31	0.34
TS3	2.19	1.25	0.56	0.23
TS4	3.00	1.24	0.56	0.26
TS5	1.62	1.24	0.25	0.22
TS6	3.15	1.27	0.21	0.34

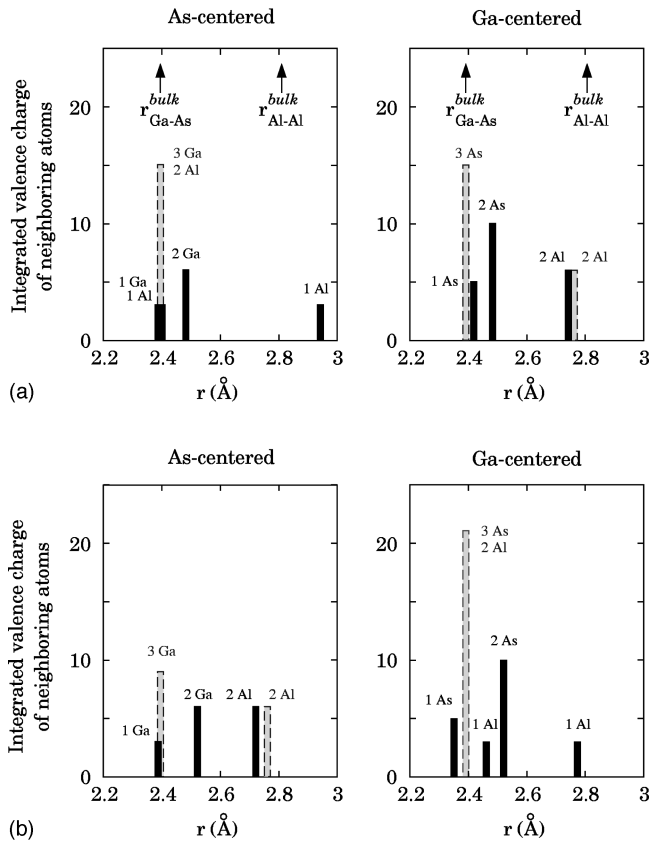


FIG. 2. Radial distribution of neighboring ions around an As ion (left panel) and around a Ga ion (right panel) of the semiconductor surface at the (a) TS1 and (b) TS2 Al/GaAs (110) interfaces. The gray bars correspond to the starting (unrelaxed) configuration and the black bars to the relaxed configuration.

In Fig. 2, we show the radial distribution of ions around each As and Ga surface atom in the TS1 and TS2 structures, before and after relaxation. In the TS1 (TS2) structure, each surface As (Ga) atom has 2 Al and 3 Ga (As) nearest neighbors at a distance equal to the Ga-As bond length in GaAs. This represents a significant overcoordination with respect to the situation in bulk GaAs (in terms of number of neighbors as well as ionic charges). After relaxation of the TS1 structure, one of the Al nearest neighbors of the As atom (the Al-II atom) has moved away from the As to a distance that exceeds the Al-Al nearest-neighbor distance in the metal. This leads to a situation in which the As atom has almost recovered its bulk coordination. After relaxation of the TS2 structure, one of the Al nearest neighbors of the Ga atom (the Al-I atom) has also moved away from the Ga. In this case, the corresponding Ga-Al separation is almost identical to the Al-Al bonding distance in the bulk-metallic phase. Because of this additional “metalliclike” bond, the remaining (short) Ga-Al bond and especially the two in-plane As-Ga bonds weaken, as indicated by the corresponding increased bond lengths in Fig. 2.

The above relaxations tend to restore a “covalent” bonding environment around each As surface atom in the TS1’ structure, and establish a configuration with mixed covalent and metalliclike Ga-Al interfacial bonds around each Ga surface atom in the TS2’ structure. In both cases, the remaining semiconductor surface atom, i.e., the TS1’ Ga atom and the

TS2’ As atom, forms long metalliclike bonds with the two neighboring Al-II atoms across the interface (Fig. 2). These different types of bonding configurations for the As and the Ga atoms tend to preserve the fcc atomic arrangement of the first layer of Al.

The TS5’ structure is intermediate between the TS1’ and TS2’ structures. In this case, two short bonds are established across the interface, one from the As to the Al-I atom (2.44 Å) and one from the Ga to the Al-II atom (2.48 Å). The second-nearest Al neighbor of the As (Ga) atom is at a distance of 3.30 Å (3.15 Å), i.e., far beyond the Al-Al interatomic distance in the metal. The formation energy of the TS5’ structure is identical to those of the TS1’ and TS2’ structures to within 30 meV per GaAs pair, which is less than  $k_B T$  per atom at room temperature. This is at the limit of our accuracy, and the three structures should therefore be considered as essentially degenerate in energy. Other TS’s intermediate between TS1’ and TS2’ in Fig. 1 are also expected to yield configurations with similarly low formation energies. This situation is in contrast to the case of the (100) junction, for which a unique equilibrium configuration was obtained for a given (As or Ga) termination of the semiconductor. The existence of quasidegenerate equilibrium interfacial configurations for the nonpolar (110) junction results from a competition between the optimization of covalentlike bonds between the anions of the semiconductor surface and selected Al (Al-I) surface atoms, and mixed covalent/metallic bonds between the cations and the Al (I and II) surface atoms.

There is a strong parallel between our results and conclusions for the fully developed Al/GaAs (110) interface and those obtained by Schmidt and Srivastava who studied one monolayer of Al absorbed on the GaAs (110) surface.<sup>38</sup> These authors also found, from *ab initio* calculations, several competing structures characterized by almost identical adsorption energies but different surface bonding configurations. Two of their most favorable Al epitaxial configurations (the As-dimer and Ga-dimer configurations) correspond to the atomic arrangement of the Al-I and Al-II ions in the TS1’ and TS2’ structures. Schmidt and Srivastava obtained two other favorable high-symmetry structures: the epitaxially continued layer structure (ECLS) and the irregular chain structure (IRC). The atomic arrangement of the Al layer in latter two configurations, however, is not compatible with that of an Al fcc lattice. In fact, with the constraint of a fully developed epitaxial overlayer, we find that the ECLS and IRC interfacial configurations do not remain energetically competitive.<sup>39</sup>

Needs *et al.* have also examined the formation energies of the six Al/GaAs (110) TS’s illustrated in Fig. 1 using an *ab initio* pseudopotential approach.<sup>22</sup> For the unrelaxed configurations, the energy ordering we obtain for the different TS’s is the same as in their study, and the formation energies agree to within 0.2 eV. For the relaxed configurations, however, our results are different. Needs *et al.* found the TS5 structure to be the lowest-energy configuration, and reported a formation-energy range of 0.5 eV per GaAs pair for the different TS’s. Although the TS5 structure is also among our lowest energy configurations, our results show that the six TS’s give rise to only three distinct (meta)stable configurations that are virtually degenerate in energy when fully re-

laxed. These discrepancies are attributed to incomplete atomic relaxation of some of the TS's in the previous study, which might be due to the low-energy cutoff (8 Ry) that was used for the relaxation.

#### IV. SCHOTTKY BARRIERS

##### A. Dependence on interface geometry

The Schottky barriers of the different Al/GaAs (100) and (110) TS's are shown in Tables I and II. In the polar Al/GaAs (100) junctions, the Schottky barrier exhibits a non-negligible dependence on the semiconductor surface termination:  $\phi_p$  is systematically higher by 0.1 to 0.2 eV at the As-terminated interface than at the Ga-terminated interface (see Table I). For the lowest-energy translation state (TS1), the  $p$ -type barrier of the As-terminated interface is 0.13 eV higher than that of the Ga-terminated interface. Lattice relaxation at the interface changes the values of the two barriers by only a few tenths of an eV, and increases the barrier difference to 0.16 eV.

We note that the (100) Schottky barrier is much less sensitive to atomic relaxation and to rigid translations of the metal overlayer than the (110) barrier. In the (100) junctions, e.g., in-plane displacements of the Al overlayer over distances as large as  $0.25a_{\parallel}$ , or even  $0.35a_{\parallel}$ , from the reference TS1 configuration (corresponding to the TS1  $\rightarrow$  TS2, TS1  $\rightarrow$  TS4, or TS1  $\rightarrow$  TS5 translation) modify the Schottky barrier height by no more than 0.02 eV. In the (110) junction, instead, similar translations of the metal by  $0.31a_{\parallel}$  from the low-energy TS5 configuration (corresponding, e.g., to the TS5  $\rightarrow$  TS1 or TS5  $\rightarrow$  TS4 translation) can change the barrier height by as much as 0.4 eV. We attribute the weaker sensitivity of the (100) barrier to changes in the interfacial geometry to the more metallic character of the polar (100) interface. In the TS1 (100) junctions, the local density of electronic states at the Fermi energy, in the region between the last semiconductor layer and the first metal layer, is about  $1.0 \text{ eV}^{-1} \Omega^{-1}$  ( $\Omega$  being the GaAs unit-cell volume), whereas it is only  $0.6 \text{ eV}^{-1} \Omega^{-1}$  in the TS5 (110) junction.

Taking into account relativistic, many-body, and Ga  $3d$  corrections (Sec. II), the theoretical values of  $\phi_p$  for the equilibrium As- and Ga-terminated TS1' interface structures are 0.80 eV and 0.64 eV, respectively. Using the experimental band-gap value of 1.42 eV for GaAs at room temperature, this yields  $n$ -type barriers of 0.62 eV and 0.78 eV for the As- and Ga-terminated interfaces, respectively. These values compare relatively well with the  $n$ -type barriers determined by transport measurements in Al/GaAs (100) junctions, which generally range between 0.7 and 0.8 eV.<sup>14,40</sup> Some transport studies also indicated a  $\sim 0.1$  eV increase in the  $n$ -type barrier for junctions fabricated on Ga-rich as compared to As-rich GaAs surfaces.<sup>15,41</sup> The increased  $n$ -type barrier for the initial Ga-rich relative to the As-rich surfaces have also been observed in photoemission experiments.<sup>42</sup> The LDA values of the  $p$ -type barrier we obtain for the relaxed TS1 interface structures are also consistent with the values computed by Dandrea and Duke.<sup>20</sup>

At the Al/GaAs (110) interface, lattice relaxation is found to modify considerably the range of Schottky barrier heights, reducing its width from  $\sim 0.5$  eV to  $\sim 0.1$  eV (Table II). This is in contrast with the results by Needs *et al.* who re-

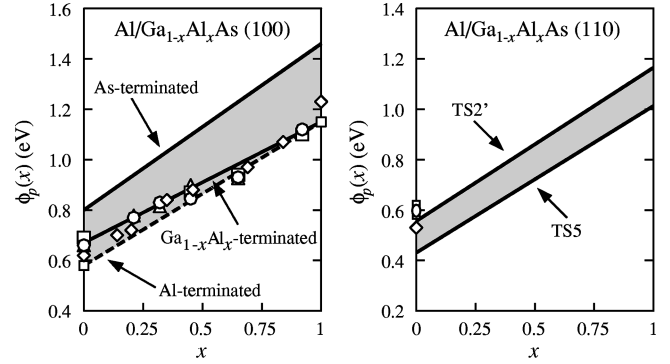


FIG. 3. Alloy-composition dependence of the Al/Ga<sub>1-x</sub>Al<sub>x</sub>As (100) and (110) Schottky barrier height  $\phi_p$  for different interfacial atomic geometries. The symbols show the experimental data from Ref. 14 [ $\diamond$ ,  $I(V)$ ] and Ref. 40 [ $\Delta$ ,  $I(V)$ ;  $\circ$ ,  $C(V)$ ;  $\square$ , IPE] for the (100) junctions, and from Ref. 43 ( $\diamond$ ), Ref. 44 ( $\square$ ), and Ref. 45 ( $\circ$ ) for the (110) junctions.

ported differences as large as 0.7 eV between the Schottky barriers of the relaxed TS's.<sup>22</sup> As mentioned before, we attribute such discrepancies to the incomplete atomic relaxation at some interfaces, in the previous study. The wide range of barrier heights found for the unrelaxed TS's correspond to systems in which unphysical bonds exist at some interfaces. Some bonds are much too short and some semiconductor atoms at the interface are overcoordinated. It is noteworthy that although our three independent relaxed interface structures (TS1', TS2', and TS5') exhibit quite different bonds across the interface, they give rise to a range of barrier heights whose width is comparable to that of the (100) barriers. It should also be noticed, however, that the barrier heights of these epitaxial (110) junctions are  $\sim 0.2$  eV smaller than those of the (100) junctions.

The theoretical values of  $\phi_p$  that we obtain for the abrupt epitaxial (110) interfaces range from 0.37 eV to 0.49 eV (including relativistic, many-body and Ga  $3d$  corrections). These values are  $\sim 0.1$  eV lower than those typically obtained from transport measurements in junctions with thick metal overlayers, where  $\phi_p$  ranges from 0.53 eV to 0.64 eV (Refs. 43–45, see Fig. 3). For other junctions, such as those produced by Al cluster deposition, a wider range of barrier heights (0.7 eV) has been reported.<sup>11</sup> It should be stressed, however, that the experimental atomic-scale structure established at these interfaces is largely unknown.

The *ab initio* calculations indicate that, unlike band offsets at isovalent semiconductor heterojunctions that were shown<sup>23</sup> to depend, most generally, only on the bulk properties of the materials forming the junction, the Schottky barrier do depend, in general, on interface-specific features, and in particular on the atomic geometry of the interface. The sensitivity to perturbations of the atomic geometry is especially striking in the case of the nonpolar (110) junctions, and consistent with the results of other recent theoretical studies.<sup>20–22</sup> We also find, however, that atomic relaxation at the interface tends to reduce significantly the physical range of barrier heights established in epitaxial Al/GaAs (110) junctions. In particular, the range of 0.7 eV that was reported from previous calculations<sup>22</sup> for abrupt epitaxial Al/GaAs (110) junctions shrinks to less than 0.2 eV when the atomic structure at the interface is fully relaxed.

## B. Compositional dependence

In Fig. 3, we show the calculated alloy-composition dependence of the Al/Ga<sub>1-x</sub>Al<sub>x</sub>As Schottky barrier height for the Ga- and As-terminated TS1 (100) junctions and for the TS5 and TS2' (110) junctions (which correspond to the low-energy TS's with the smallest and largest Schottky barrier heights). These calculations were performed using for the Al/Ga<sub>1-x</sub>Al<sub>x</sub>As junctions the same structural parameters as for the Al/GaAs junctions. Lattice relaxation at the Al/AlAs interface changes  $\phi_p$  by at most 50 meV. Even though the absolute value of  $\phi_p$  is different for the different interface atomic structures and orientations, the variation of the barrier with alloy composition is relatively similar for the various interfaces considered in Fig. 3. This is consistent with the results of other computations performed for the As-terminated TS1 (100) and the TS1 (110) interfaces.<sup>46</sup> In Fig. 3, we also show the available experimental data on the alloy-composition dependence of the Al/Ga<sub>1-x</sub>Al<sub>x</sub>As (100) Schottky barrier. For the (110) interface, no experimental data are available yet for compositions  $x > 0$ . Taking into account the estimated theoretical uncertainty of 0.1 eV on the absolute value of  $\phi_p$ , and the unknown structural details and exact stoichiometry of the experimental interfaces, good general agreement is found between the theoretical and experimental trends.

Experimentally, the band discontinuities at the Al/GaAs, Al/AlAs, and GaAs/AlAs (100) interfaces verify the transitivity rule within experimental uncertainty: the difference  $\Delta\phi_p = \phi_p(\text{AlAs}) - \phi_p(\text{GaAs})$  ranges from 0.45 to 0.6 eV, and the band offset VBO (GaAs/AlAs) from 0.45 to 0.55 eV.<sup>47</sup> In our calculations, the transitivity rule is verified to within a few tenths of meV for the As-terminated TS1 (100) junctions and for the TS5 and TS2' (110) junctions: the corresponding LDA values for  $\Delta\phi_p$  range from 0.42 to 0.49 eV, and the LDA value of the VBO is 0.49 eV (see the Appendix). The many-body, spin-orbit, and Ga 3d corrections<sup>48</sup> described in Sec. II apply to bulk values, and do not affect the transitivity properties. In the case of the cation-terminated (100) interface, we find a larger deviation from the transitivity rule:  $\sim 0.2$  eV, which is related to the fact that this is the interface where the composition within the semiconductor layer in contact with the metal changes the most with  $x$ .

It should be noted in this connection, and when comparing with experiment, that a Ga-Al exchange reaction yielding excess AlAs near the interface is known to take place in Al/GaAs (100) junctions.<sup>49</sup> In fact, from total-energy calculations, we find that a substitution of the Ga atoms by Al atoms in the Ga plane adjacent to the interface lowers the formation energy of the cation-terminated (100) junction by 0.7 eV for  $\mu_{\text{As}} = \mu_{\text{As}}^{\text{bulk}}$  (upper bound of the As chemical potential). The same substitution increases the formation energy by less than 0.1 eV for the lower bound of  $\mu_{\text{As}}$  ( $\mu_{\text{As}} = \mu_{\text{GaAs}} - \mu_{\text{Ga}}^{\text{bulk}}$ ).<sup>50</sup> Such a substitution is therefore energetically favorable in most of the physically allowed range of  $\mu_{\text{As}}$ . The Ga-Al exchange reaction, driven by the large heat of formation of AlAs, is expected to occur experimentally also in Al/Ga<sub>1-x</sub>Al<sub>x</sub>As (100) junctions with  $0 < x < 1$ . When the calculations of the Schottky barriers are performed for cation-terminated Al/Ga<sub>1-x</sub>Al<sub>x</sub>As (100) junctions in-

cluding one (or more) AlAs bilayer(s) at the interface, the deviation from the transitivity rule decreases to a few tenths of meV, and the barrier variation with alloy composition becomes similar to those found for the other interfaces (see Fig. 3). We note that somewhat similar results were also obtained from full-potential linearized augmented-plane-wave calculations for cation-terminated Al/GaN (100) junctions. The Ga-Al exchange reaction was found to be exothermic, and the Schottky barriers of junctions including AlN interlayers were found to exhibit only very small deviations from the transitivity rule.<sup>51</sup>

## C. Linear-response approach

In the case of semiconductor heterojunctions, an approach based on linear-response theory (LRT) showed that the band offset in isovalent heterojunctions, such as GaAs/AlAs, depends only on the bulk properties of the semiconductor constituents.<sup>23</sup> Here we will use a similar approach, focusing on the properties of the charge density in the junctions, to explain the Schottky-barrier trends with semiconductor alloy composition and the link with heterojunction band offsets.

Similarly to the Schottky barrier in Eq. (1), the band offset is conveniently split into two contributions:  $\Delta E_v + \Delta V$ . The first term is the band-structure term, which is equal to the difference between the valence-band-edge energies measured with respect to the average electrostatic potential in the two semiconductors, and the second term is the electrostatic potential lineup at the interface. Since the band-structure terms are bulk quantities, and verify, by definition, the transitivity rule, the potential lineups are the main focus here.

Within the LRT approach,<sup>23</sup> a semiconductor heterojunction such as GaAs/AlAs is considered as a perturbation with respect to an appropriate bulk reference, which may be chosen as one of the two semiconductors, e.g., GaAs. The perturbation that builds up the GaAs/AlAs interface amounts to replacing all Ga ions by Al ions on one side of the GaAs/GaAs homojunction. The charge density induced by this perturbation, which is responsible for the lineup  $\Delta V(\text{GaAs/AlAs})$ , is given, to the first order, by a superposition of charge densities induced by single Ga  $\rightarrow$  Al atomic (or atomic-plane) substitutions in bulk GaAs. The corresponding potential lineup reads

$$\begin{aligned} \Delta V &= -\frac{2\pi e^2}{L^\alpha} \int z^2 \Delta n_{\text{bulk}}^\alpha(z) dz \\ &= -\frac{2\pi e^2}{3\Omega} \int r^2 \Delta \hat{n}_{\text{bulk}}(\mathbf{r}) d\mathbf{r}, \end{aligned} \quad (5)$$

where  $L$  is the distance between two consecutive cations planes in the junction,  $\alpha$  refers to the interface orientation,  $\Omega$  is the volume of the bulk unit cell, and  $\Delta \hat{n}_{\text{bulk}}(\mathbf{r})$  [ $\Delta n_{\text{bulk}}(z)$ ] is the (planar-averaged) charge-density induced by the single Ga  $\rightarrow$  Al (atomic) atomic-plane substitution in bulk GaAs. For the GaAs/AlAs system, the lineup calculated within LRT is identical, to within 0.02 eV, to the result obtained from full self-consistent supercell calculations.<sup>28</sup> The LRT results [Eq. (5)] show that the lineup is determined only by bulk quantities, and is the same for all interface orientations.

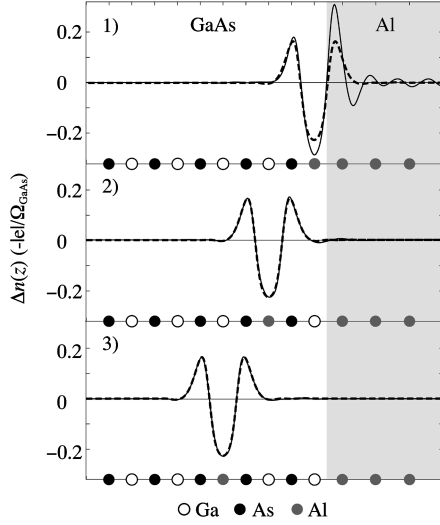


FIG. 4. Planar average of the valence-charge density induced by Ga  $\rightarrow$  Al single-plane substitutions in the Ga-terminated TS1 Al/GaAs (100) junction. The plane-averaged charge density induced by a Ga  $\rightarrow$  Al (100) single-plane substitution in bulk GaAs is also shown for comparison (dashed line).

In a similar way, we consider the Al/AlAs junction as a perturbation with respect to the Al/GaAs junction. We then construct the charge density of the Al/AlAs interface, starting from the Al/GaAs interface, by adding a linear superposition of the charge-density responses to single Ga  $\rightarrow$  Al atomic-plane substitutions in the semi-infinite semiconductor region. We note that an ideal linear superposition of the bulk semiconductor responses  $\Delta n_{\text{bulk}}(z)$  in that region would induce a change in the potential lineup across the interface identical to  $\Delta V(\text{GaAs}/\text{AlAs})$  in Eq. (5), that would satisfy the transitivity rule. The actual response,  $\Delta n_i(z)$ , to the substitution of the  $i$ th cation layer from the Al/GaAs interface must coincide with  $\Delta n_{\text{bulk}}(z)$  for large  $i$ . The nonbulk contribution,  $\Delta V_{\text{diff}}$ , to the potential lineup, which is responsible for the deviation from the transitivity rule

$$\phi_p(\text{Al}/\text{AlAs}) - \phi_p(\text{Al}/\text{GaAs}) = \Delta E_{\text{VBO}}(\text{AlAs}/\text{GaAs}) + \Delta V_{\text{diff}}, \quad (6)$$

derives thus from the polarization of the  $\Delta n_i(z)$  near the interface.

In Figs. 4 and 5, we compare the response  $\Delta n_i(z)$  to the bulk response  $\Delta n_{\text{bulk}}(z)$  for substitutions performed within the first three cation layers from the interface in the Ga-terminated Al/GaAs (100) junction and in the TS5 Al/GaAs (110) junction. Except for the substitution performed

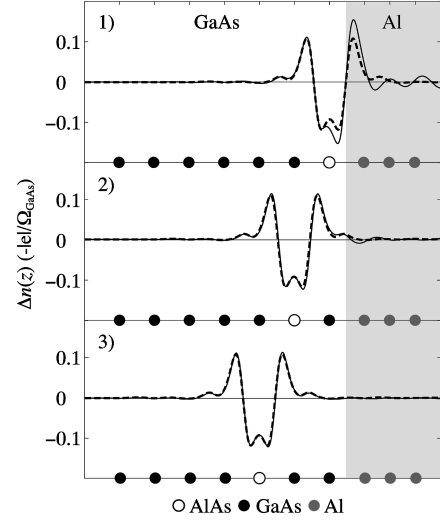


FIG. 5. Planar average of the valence-charge density induced by Ga  $\rightarrow$  Al single-plane substitutions in the TS5 Al/GaAs (110) junction. The plane-averaged charge density induced by a Ga  $\rightarrow$  Al (110) single-plane substitution in bulk GaAs is also shown for comparison (dashed line).

within the plane adjacent to the metal, the other substitutions give rise to charge profiles  $\Delta n_i(z)$  very similar to the bulk result. The presence of the metal can be seen to induce some asymmetry in the response, which decreases rapidly with  $i$ . Assuming thus a linear superposition of the  $\Delta n_i(z)$  in the semiconductor region, the deviation from the transitivity rule is given by

$$\Delta V_{\text{diff}}^{\text{LRT}} = \sum_i d_i, \quad (7)$$

where

$$d_i = 4\pi e^2 \int z \Delta n_i(z) dz \quad (8)$$

are the microscopic dipoles induced by the asymmetric  $\Delta n_i(z)$  near the junction. In Table III, we reported the values of  $\Delta V_{\text{diff}}$  and of the dipoles  $d_i$  for the As- and Ga-terminated (100) junctions and for the TS5 (110) junction.<sup>52</sup> The dipoles  $d_i$  vanish beyond the fourth cation plane from the interface. The results in Table III show that this LRT approach accounts for most of the deviation from the transitivity rule. The remaining difference is comparable to our numerical uncertainty.

This atomic scale study allows one thus to understand, in terms of the microscopic properties of the charge density in

TABLE III. Dipoles  $d_i$  (in eV) induced by Ga  $\rightarrow$  Al single-layer substitutions performed within the first few cation layers  $i$  ( $i=1, \dots, 4$ ) from the metal in Al/GaAs (100) and (110) junctions. The dipoles are negligible beyond the fourth cation layer.  $\Delta V_{\text{diff}}$  is the deviation (in eV) from the transitivity rule as calculated from Eq. (6).

Interface Al/GaAs	$d_1$	$d_2$	$d_3$	$d_4$	$\Sigma_i d_i$	$\Delta V_{\text{diff}}$
(100) As-term.	+0.05	-0.04	-0.01	0.00	0.00	0.00
(100) Ga-term.	-0.09	-0.04	-0.03	0.00	-0.16	-0.18
(110) TS5	+0.01	-0.04	-0.03	-0.02	-0.08	-0.05



the junctions, the observed correlation between band-offset and Schottky-barrier trends. The results show that the variation of the lineup with the alloy composition can be decomposed into two contributions. A first (dominant) bulk contribution depends only on the semiconductor material, and is related to the charge-density building blocks emphasized in the LRT description of the band offsets. This contribution is always present and leads to transitive properties of the band discontinuities. The second contribution is interface related, accounts for the deviation from the transitivity rule, and derives from local dipoles induced by changes in the semiconductor composition within essentially the last semiconductor layer in contact with the metal. For the Al/Ga<sub>1-x</sub>Al<sub>x</sub>As system, this contribution was found to be relevant only in the case of the cation-terminated (100) junction. Moreover, we showed that the Ga-Al exchange reaction, which is known to take place experimentally in Al/GaAs junctions, tends to reduce this contribution.

## V. CONCLUSIONS

Using an *ab initio* approach, we examined the atomic and electronic structures of chemically abrupt epitaxial Al/GaAs and Al/Ga<sub>1-x</sub>Al<sub>x</sub>As (100) and (110) junctions, and investigated the dependence of the corresponding Schottky barrier height on the interface geometry and semiconductor alloy composition. For the prototype Al/GaAs system, our calculations showed a unique equilibrium epitaxial geometry of the polar (100)-oriented interface for a given cation or anion termination of the semiconductor surface. For the nonpolar (110) interface, instead, we obtained competing structures with different interfacial bonds. This diversity results from a competition between the optimization of covalentlike bonds, involving the anions of the semiconductor surface and selected Al surface atoms, and metalliclike bonds involving the cations and the Al surface atoms.

Our results concerning the electronic properties of these systems showed that, depending on the atomic structures and orientation of the interface, the absolute value of the Schottky barrier can change by as much as 0.4 eV. However, for a given equilibrium interfacial atomic geometry, the Al/Ga<sub>1-x</sub>Al<sub>x</sub>As(100) and (110) junctions exhibit similar barrier variations with semiconductor alloy composition  $x$ , amounting to the GaAs/Ga<sub>1-x</sub>Al<sub>x</sub>As band offset. This trend is not substantially affected by deviations from the bulk stoichiometry in the interfacial region, and was explained on the atomic scale by extending to metal/semiconductor interfaces a linear-response approach employed in the study of band offsets.

## ACKNOWLEDGMENTS

We would like to acknowledge support for this work by the Swiss National Science Foundation under Grant No. 20-47065.96. Computations were performed at EPFL in Lausanne and at the CSCS in Manno.

## APPENDIX: ROLE OF THE Ga 3d ELECTRONS

In this appendix, we discuss the effect of the Ga 3d electrons on the Al/GaAs(100) Schottky barrier and on the GaAs/AlAs(100) band offset, and its impact on the transitivity

TABLE IV. LDA values of the Al/GaAs(100)  $p$ -type Schottky barrier height ( $\phi_p$ ) and of the AlAs/GaAs(100) valence-band offset  $\Delta E_{\text{VBO}}$  for different treatments of the Ga 3d states, namely, as core states with and without the nonlinear core correction (nlcc) and as valence states. The Schottky barrier has been calculated for the As-terminated TS1 interface structure illustrated in Fig. 1. All energies are in eV.

Ga 3d	$a_{\text{GaAs}} = 5.53 \text{ \AA}$		$a_{\text{GaAs}} = 5.59 \text{ \AA}$	
	$\phi_p^{(\text{LDA})}$	$\Delta E_{\text{VBO}}$	$\phi_p^{(\text{LDA})}$	$\Delta E_{\text{VBO}}$
Core states	0.64	0.50	0.58	0.47
Core states with nlcc	0.62	0.53	0.56	0.50
Valence states	0.59	0.56	0.53	0.53

properties of the band discontinuities at the Al/GaAs, GaAs/AlAs, and Al/AlAs interfaces. Our calculations were performed in two steps. The Ga 3d states were first treated as frozen core orbitals, and we used a nonlinear core correction for the exchange-correlation potential<sup>53</sup> which partially takes into account the effects of the Ga 3d electrons. We then carried out the full calculations, including also the relaxation of the semicore orbitals, by treating the Ga 3d states as valence states. The latter calculations were performed with Troullier-Martins pseudopotentials using a plane-wave-energy cutoff of 100 Ry. The computations of the GaAs/AlAs(100) band offset were performed with a 6+6 supercell using a (6, 6, 2) MP grid. The other computational details are as given in Sec. II. The results for the Al/GaAs Schottky barrier and GaAs/AlAs VBO are listed in Table IV.

We separated the effect of the Ga 3d electrons into two contributions related to changes in the structural parameters and in the chemistry (see Table IV). The first effect takes into account the increase in the GaAs equilibrium lattice constant,  $a_{\text{GaAs}}$ , from 5.53 to 5.59 Å, which occurs when the Ga 3d electrons are treated as valence electrons instead of core electrons. Changing only the lattice parameter and keeping the Ga 3d electrons in the core (or in the valence) lowers the Al/GaAs Schottky barriers  $\phi_p$  by 0.06 eV and the AlAs/GaAs valence band offset by 0.03 eV (using the same lattice parameter for GaAs and AlAs). The same variation from 5.53 to 5.59 Å in the AlAs lattice parameter would reduce the Al/AlAs Schottky barrier  $\phi_p^{(\text{LDA})}$  from 1.14 eV to 1.09 eV, i.e., by 0.05 eV. These changes are consistent (to within our numerical accuracy) with the variations one would predict based on the volume change (+3.2%) and hydrostatic deformation potentials of GaAs and AlAs:<sup>54</sup>  $\Delta\phi_p(\text{Al/GaAs}) = -0.04 \text{ eV}$ ,  $\Delta\phi_p(\text{Al/AlAs}) = -0.05 \text{ eV}$ , and  $\Delta V_{\text{VBO}}(\text{GaAs/AlAs}) = +0.01 \text{ eV}$ . These variations are therefore controlled essentially by the bulk properties of the semiconductors.

The second effect corresponds to the inclusion, at fixed geometry, of the Ga 3d states among the valence states. Performing this change at  $a_{\text{GaAs}} = 5.59 \text{ \AA}$  (or 5.53 Å) lowers the Schottky barrier  $\phi_p(\text{Al/GaAs})$  by 0.05 eV and increases the band offset  $\Delta E_{\text{VBO}}(\text{AlAs/GaAs})$  by almost the same amount, i.e., 0.06 eV. This 0.06 eV increase in the AlAs/GaAs VBO is exactly equal to the VBO we obtain at a GaAs/GaAs(100) homojunction in which the Ga 3d electrons are treated as core electrons on one side of the junction and as

valence electrons on the other side of the junction. The chemical effect of the Ga 3*d* electrons can be considered thus as a bulklike correction that raises the GaAs valence-band edge by about the same amount in all cases.

Because of the bulklike nature of the above effects, the Ga 3*d*-related corrections do not affect the transitivity properties of the band discontinuities at the Al/GaAs, GaAs/AIAs and Al/AIAs interfaces by more than our numerical uncertainty, i.e., 0.04 eV. We note that for the Al/GaAs Schottky barrier the structural and chemical corrections add up, yield-

ing a total correction of  $\sim 0.1$  eV, whereas in the case of the GaAs/AIAs VBO the structural contribution resulting from the AIAs volume change partially cancels out the GaAs-related corrections, yielding a total change of only 0.03 eV. Finally, we would like to note that the nonlinear-core correction correctly reproduces the change from 5.53 to 5.59 Å in the GaAs lattice parameter and the related structural corrections on the band discontinuities, but accounts for only 50% of the chemical correction on  $\phi_p(\text{Al/GaAs})$  and on  $\Delta E_{\text{VBO}}(\text{GaAs/AIAs})$ .

- 
- <sup>1</sup>L. J. Brillson, in *Handbook on Semiconductors*, edited by P. T. Landsberg (North-Holland, Amsterdam, 1992), Vol. 1, p. 281.
- <sup>2</sup>V. Heine, Phys. Rev. **138**, A1689 (1965).
- <sup>3</sup>J. Tersoff, Phys. Rev. Lett. **52**, 465 (1984).
- <sup>4</sup>F. Flores and C. Tejedor, J. Phys. C **20**, 145 (1987); F. Guinea, J. Sánchez-Dehesa, and F. Flores, *ibid.* **16**, 6499 (1983).
- <sup>5</sup>W. Spicer, Semicond. Semimet. **38**, 449 (1993).
- <sup>6</sup>J. M. Woodall and J. L. Freeouf, J. Vac. Sci. Technol. **21**, 574 (1982).
- <sup>7</sup>G. Margaritondo and P. Perfetti, in *Heterojunction Band Discontinuities*, edited by F. Capasso and G. Margaritondo (North-Holland, Amsterdam, 1987), p. 59.
- <sup>8</sup>C. J. Palmström and T. D. Sands, in *Contacts to Semiconductors*, edited by L. J. Brillson (Noyes, Park Ridge, 1993), p. 67.
- <sup>9</sup>J.-K. Lee, Y.-H. Cho, B.-D. Choe, K. S. Kim, H. I. Jeon, H. Lim, and M. Razeghi, Appl. Phys. Lett. **71**, 912 (1997).
- <sup>10</sup>J. Tersoff, Phys. Rev. B **30**, 4874 (1984).
- <sup>11</sup>G. D. Waddill, I. M. Vitomirov, C. M. Aldao, S. G. Anderson, C. Capasso, J. H. Weaver, and Z. Liliental-Weber, Phys. Rev. B **41**, 5293 (1990).
- <sup>12</sup>L. J. Brillson, I. M. Vitomirov, A. Raisanen, S. Chang, R. E. Viturro, P. D. Kirchner, G. D. Pettit, and J. M. Woodall, Appl. Surf. Sci. **65/66**, 667 (1993).
- <sup>13</sup>M. Cantile, L. Sorba, S. Yildirim, P. Faraci, G. Biasiol, A. Franciosi, T. J. Miller, and M. I. Nathan, Appl. Phys. Lett. **64**, 988 (1994).
- <sup>14</sup>M. Missous, W. S. Truscott, and K. E. Singer, J. Appl. Phys. **68**, 2239 (1990).
- <sup>15</sup>A. Y. Cho and P. D. Dernier, J. Appl. Phys. **49**, 3328 (1978).
- <sup>16</sup>G. Landgren, R. Ludeke, and C. Serrano, J. Cryst. Growth **60**, 393 (1982).
- <sup>17</sup>G. A. Prinz, J. M. Ferrari, and M. Goldenberg, Appl. Phys. Lett. **40**, 155 (1982).
- <sup>18</sup>S. B. Zhang, M. L. Cohen, and S. G. Louie, Phys. Rev. B **34**, 768 (1986).
- <sup>19</sup>M. van Schilfgaarde and N. Newman, Phys. Rev. Lett. **65**, 2728 (1990).
- <sup>20</sup>R. G. Dandrea and C. B. Duke, J. Vac. Sci. Technol. A **11**, 848 (1993); J. Vac. Sci. Technol. B **11**, 1553 (1993).
- <sup>21</sup>A. Ruini, R. Resta, and S. Baroni, Phys. Rev. B **56**, 14 921 (1997).
- <sup>22</sup>R. J. Needs, J. P. A. Charlesworth, and R. W. Godby, Europhys. Lett. **25**, 31 (1994).
- <sup>23</sup>S. Baroni, R. Resta, A. Baldereschi, and M. Peressi, in *Spectroscopy of Semiconductor Microstructures*, Vol. 206 of *NATO Advanced Study Institutes Series B: Physics*, edited by G. Fasol, A. Fasolino, and P. Luigi (Plenum, New York, 1989), p. 251; A. Baldereschi, M. Peressi, S. Baroni, and R. Resta, in *Semiconductor Superlattices and Interfaces*, Proceedings of the International School of Physics "Enrico Fermi," Course CXVII, Varenna, 1991, edited by A. Stella and L. Miglio (North-Holland, Amsterdam, 1993), p. 59.
- <sup>24</sup>N. Troullier and J. L. Martins, Phys. Rev. B **43**, 1993 (1991).
- <sup>25</sup>L. Kleinman and D. M. Bylander, Phys. Rev. Lett. **48**, 1425 (1982).
- <sup>26</sup>D. M. Ceperley and B. J. Alder, Phys. Rev. Lett. **45**, 566 (1980); J. P. Perdew and A. Zunger, Phys. Rev. B **23**, 5048 (1981).
- <sup>27</sup>J. Ihm, A. Zunger, and M. L. Cohen, J. Phys. C **12**, 4409 (1979); **13**, 3095 (1980).
- <sup>28</sup>See, e.g., M. Peressi, N. Binggeli, and A. Baldereschi, J. Phys. D **31**, 1273 (1998).
- <sup>29</sup>C.-L. Fu and K.-M. Ho, Phys. Rev. B **28**, 5480 (1983).
- <sup>30</sup>C. Berthod, J. Bardi, N. Binggeli, and A. Baldereschi, J. Vac. Sci. Technol. B **14**, 3000 (1996).
- <sup>31</sup>S. B. Zhang, D. Tománek, S. G. Louie, M. L. Cohen, and M. S. Hybertsen, Solid State Commun. **66**, 585 (1988).
- <sup>32</sup>N. D. Lang and W. Kohn, Phys. Rev. B **3**, 1215 (1971); W. Kohn, *ibid.* **33**, 4331 (1986).
- <sup>33</sup>C. J. Fall, N. Binggeli, and A. Baldereschi, Phys. Rev. B **58**, R7544 (1998).
- <sup>34</sup>A shift of  $-0.14$  eV was reported in Ref. 22 from the self-energy calculations for the Al Fermi energy. However, because of the above arguments, and also because of the relatively large (0.1–0.2 eV) uncertainties of many-body corrections resulting from different *ab initio* calculations, we decided to use the LDA-DFT result in the present study. We note that a different choice was made in Ref. 54.
- <sup>35</sup>R. F. S. Hearmon, in *Elastic, Piezoelectric and Related Constants of Crystals*, edited by K. H. Hellwege and A. M. Hellwege, Landolt-Börnstein, New Series, Group III, Vol. 11 (Springer, Berlin, 1979), p. 109.
- <sup>36</sup>For the low symmetry TS4 (TS $\bar{4}$ ) geometries, the (100) supercell contains a pair of TS4-TS $\bar{4}$  interfaces [because of the lack of (100) reflection symmetry of the Al/GaAs/Al(100) supercells]. The formation energy reported in the table is therefore an average of the TS4 and TS $\bar{4}$  formation energies. The TS4 and TS $\bar{4}$  formation energies could be determined separately from calculations using a vacuum/Al/GaAs/Al/vacuum heterostructures. However, given the highly unfavorable formation energy of the coupled interfaces, these values were not determined here. We determined, instead, the values of  $\phi_p$  for the TS4 and TS $\bar{4}$  interfaces separately (reported in the table) using a symmetric Al/

- GaAs/Al/GaAs/Al  $2 \times (13+7)$  supercell including four interfaces: TS4-TS $\bar{4}$ -TS $\bar{4}$ -TS4.
- <sup>37</sup>By symmetry, the atoms in the TS1, TS2, TS4, and TS6 (110) structures must relax within the Al(001) plane in Fig. 1.
- <sup>38</sup>W. G. Schmidt and G. P. Srivastava, *J. Phys. C* **5**, 9025 (1993).
- <sup>39</sup>When the ions of the first Al layer occupy the ECLS/IRC atomic sites, the lowest-energy translation state we obtain corresponds to a TS1 configuration for the second Al layer. The formation energy of the corresponding relaxed interface exceeds, however, by more than 0.5 eV that of the TS1' structure.
- <sup>40</sup>P. Revva, J. M. Langer, M. Missous, and A. R. Peaker, *J. Appl. Phys.* **74**, 416 (1993).
- <sup>41</sup>W. I. Wang, *J. Vac. Sci. Technol. B* **1**, 574 (1983).
- <sup>42</sup>I. M. Vitomirov, A. Raisanen, L. J. Brillson, P. D. Kirchner, G. D. Pettit, and J. M. Woodall, *J. Electron. Mater.* **22**, 309 (1993).
- <sup>43</sup>P. Phatak, N. Newman, P. Dreszer, and E. R. Weber, *Phys. Rev. B* **51**, 18 003 (1995).
- <sup>44</sup>A. B. McLean and R. H. Williams, *J. Phys. C* **21**, 783 (1988).
- <sup>45</sup>N. Newman, M. van Schilfgaarde, T. Kendelwicz, M. D. Williams, and W. E. Spicer, *Phys. Rev. B* **33**, 1146 (1986).
- <sup>46</sup>A. Ruini, Master thesis, International School for Advanced Studies, Trieste, 1995.
- <sup>47</sup>M. Missous, in *Properties of Aluminium Gallium Arsenide*, edited by S. Adachi, EMIS Datareview Series No. 7 (INSPEC, London, 1993).
- <sup>48</sup>The correction due to many-body, spin-orbit and Ga 3*d* effects (including the volume change) to the GaAs LDA VBO amounts to +0.15 eV.
- <sup>49</sup>S. A. Chambers, *Phys. Rev. B* **39**, 12 664 (1989).
- <sup>50</sup>Our values of the chemical potentials for the bulk metallic phases are  $\mu_{\text{As}}^{\text{bulk}} = -173.81$  eV,  $\mu_{\text{Ga}}^{\text{bulk}} = -61.51$  eV, and  $\mu_{\text{Al}} = -57.07$  eV (strained conditions), and for the semiconductor we have  $\mu_{\text{GaAs}} = -236.11$  eV. The change in the formation energy due to the Ga  $\rightarrow$  Al planar substitutions was evaluated neglecting the effect of atomic relaxation.
- <sup>51</sup>S. Picozzi, A. Continenza, S. Massidda, A. J. Freeman, and N. Newman, *Phys. Rev. B* **58**, 7906 (1998).
- <sup>52</sup>A similar analysis can be performed using as a reference the Al/Ga<sub>1/2</sub>Al<sub>1/2</sub>As junction. This was done in Ref. 54 for the As-terminated (100) junction, where we evaluated the dipoles  $d_i^{\text{Al(Ga)}}$  induced by single-plane Ga<sub>1/2</sub>Al<sub>1/2</sub> $\rightarrow$ Al (Ga<sub>1/2</sub>Al<sub>1/2</sub> $\rightarrow$ Ga) substitutions in the Al/Ga<sub>1/2</sub>Al<sub>1/2</sub>As junction. In that case the deviation from the transitivity rule was given by  $\sum_i d_i^{\text{Al}} - d_i^{\text{Ga}}$ .
- <sup>53</sup>S. G. Louie, S. Froyen, and M. L. Cohen, *Phys. Rev. B* **26**, 1738 (1982).
- <sup>54</sup>J. Bardi, N. Binggeli, and A. Baldereschi, *Phys. Rev. B* **54**, R11 102 (1996).